NTNU – Trondheim
Norwegian University of
Science and Technology

Variability of the Quasi Two-Day Wave in the Mesosphere

Eirik Mongstad

Teacher Education with Master of Science
Submission date: December 2013
Supervisor: Patrick Joseph Espy, IFY

Norwegian University of Science and Technology
Department of Physics

Acknowledgement

Thanks a lot to my supervisor Patrick Joseph Espy, which always have time for broad explanation of all kinds of concepts and important tips on how to structure things. Furthermore a thank you to my wife Helene for pizza delivery at my reading room and broad support through the entire progress. Finally a thank you to Bård on the desk on my right, you are always there, literally.

Abstract

The Quasi-Two-Day-Wave (QTDW) is examined through analysis of data given by the SKiYMET-radar at Dragvoll, Trondheim ($63°N, 10°E$). Through spectral analysis the occurrence and generation mechanisms of the different wave modes in the QTDW is examined. In winter, the Sudden Stratospheric Warming (SSW) event disturbs the normal solstice conditions, weakening the wind and contributes to an enhancement of all wave modes in early january. The recovered, but enhanced winter conditions with strong instabilities at high altitudes amplifies the W3-mode. At summer solstice the intensification of the near-resonant W3-mode above 90km is found to be related to the dissipation of the semi-diurnal tide in that region.

Kvasi-to-dagers bølgen (QTDW) undersøkes nærmere gjennom analyse av data produsert av SKiYMET-radaren på Dragvoll, Trondheim ($63°N, 10°E$). Gjennom spektralanalyse skal forekomstene og dannelsesmekanismer av bølgetypene i QTDW studeres. Vinterstid blir forsterkingen av alle bølgetypene knyttet til den plutselige stratosfæriske oppvarmingen (SSW) som svekket den stratosfæriske jetstrømmen og bidro til en sterkere transmisjon av forskjellige bølgetyper. Ved sommersolverv intensiveres den bølgetypen med bølgenummer 3 (W3) over 90km, og dette knyttes til spredningen av den halvdags atmosfæriske flodbølgen som følge av den sterke temperaturgradienten i det vertikale over den stratosfæriske jetstrømmen.

Contents

1 Introduction **2**

2 Theory **4**

2.1 The Atmosphere 4

2.2 Wind 4

2.3 Wave systems - Origins and behaviour 6

2.3.1 Gravity waves 6

2.3.2 Tidal waves 7

2.3.3 Planetary Waves 8

2.4 Spectral analysis 12

3 The SKiYMET radar **15**

3.1 How it works 15

4 Analysis and results **17**

4.1 Data processing in MatLab 17

4.2 Seasonal occurrence 18

4.2.1 Amplitude vs frequency 20

4.2.2 Occurrence as a function of height and time 22

5 Conclusion and further work **24**

Appendix A Figures **26**

Chapter 1

Introduction

Planetary waves in the atmosphere account for about 20% of the total power of atmospheric motion (Pancheva, 2000), so their importance cannot be neglected. The dynamics and interactions of different motions in the atmosphere are complex, and even though there is much focus on the wavemotions, there is still open questions, especially at higher latitudes. It exists several descriptions of different generation and forcing mechanisms for the Quasi Two-Day Wave (QTDW) (e.g. Plumb, 1982; Baumgaertner et al., 2008; Salby and Callaghan, 2000) and even though there is a general agreement between modes and observations, there is still need for detailed data from locations around the globe in order to get the best possible understanding of the QTDWs nature. The QTDW is a prominent feature in planetary wave family and consists of several wavemodes which have periods close to 2 days. The different components (with wavenumbers 3 and 4 being the strongest) gives the wave its characteristic variability in both period and amplitude.

While a number of climatological studies have led to a broad understanding of the Quasi Two-Day Wave (QTDW), few have investigated the variation in amplitude as the wave varies in frequency. By retrieving hourly data from the SKiYMET-radar at Dragvoll, Trondheim ($63°N, 10°E$), from October 2012 through September 2013, the relation between the QTDWs frequency and amplitude is investigated. By applying spectral analysis the aim in this thesis is to examine how different wave-generation mechanisms occur through winter and summer solstice, and to see if there are evidence of the coupling of the semi-diurnal tide dissipation with the 2-day component of the QTDW.

If the QTDW is being generated by instabilities mechanisms, both the W3 and to a certain extent the W4 component should be the most prominent components, and we would expect this to occur near solstice as the prominence of a strong temperature gradient in the vertical causes instability conditions (Baumgaertner et al., 2008). The wave is expected

to show up as a relatively stable wave during these periods, while around equinoxes, an amplitude minimum is expected. If the QTDW is being forced by tidal energy, the amplification should take place at higher altitudes where the tidal waves dissipate and redistribute their energy into the surroundings due to the strong vertical shear.

The following chapter will present some useful background theory about the atmospheric waves, paying attention to the generation and propagating mechanisms of the planetary waves and especially the QTDW. The choice of methods in the spectral analysis will be discussed briefly, before we take a look at the data source, namely the SKiYMET-radar in chapter 3. In chapter 4 the results of the analysis are presented and discussed. And finally the paper concludes in chapter 5 with a summary and a conclusion and some remarks of further interesting fields to investigate.

Chapter 2

Theory

2.1 The Atmosphere

Our atmosphere can be divided into several layers depending mostly on temperature. The following description of the atmosphere is extracted from Liou (2002). The Troposphere starts out as the warmest and stretches from ground up to about 12km decreasing its temperature along the way at a rate of $\sim -6.5\text{Kkm}^{-1}$ until it reaches the Tropospause, the point at which the temperaturegradient becomes constant with height. Above this, the stratosphere is characterized by an isothermal region that streches upwards to about 20km, above which the temperature increases. This is due to the strong absorption of UV radiation by the ozone layer in the stratosphere. When passing 50km the temperature decreases until you are at about 85km, and this region is called the Mesosphere. Most of the absorption of the solar radiation takes place in the Stratosphere, as well as some in the lower Mesosphere, and this region is dominated by radiative cooling and dynamics.

2.2 Wind

To fully understand the behaviour of the QTDW and the atmospheric wind in general, we will have to take a look at how the winds in the different parts of the atmosphere are generated and how they behave.

Describing complex windsystems on planetary scales both requires and allows us to do some approximations. When analysing the behaviour of the gas in the atmosphere we can assume it behaves like an uniform gas and follows the Perfect Gas Law

$$pV_m = RT \tag{2.1}$$

where p is the pressure, V_m is the volume of one mole of gas, R is the universal gas constant and T is the absolute temperature. The perfect gas law assumes monoatomic gases and does not take into account the interaction between the molecules in the gas since it also assumes that the distance between them is to large for any interaction to occur, which is true for gases with relatively high temperature and low density (Zumdahl and DeCoste, 2013).

The next assumption we are making is that we have hydrostatic balance, meaning that the net forces acting on any small portion of air balance each other. That is, the pressure force pushing upwards must balance the gravity force dragging parcels of air downwards. This is expressed as:

$$\frac{\partial p}{\partial z} = -g\rho. \tag{2.2}$$

with p being the pressure, z the vertical component, g the gravitational force and ρ the density.

Finally and most importantly we must assume geostrophic balance. Due to the Coriolis force, any wind moving in the meridional direction will rapidly be bent off into a zonal direction. When this happens the pressure gradient force is equal and opposite to the Coriolis force, or in other words, the winds are in geostrophic balance. The geostrophic approximation can be expressed as:

$$-fu = \frac{1}{\rho}\frac{\partial p}{\partial y} \tag{2.3a}$$

$$fv = \frac{1}{\rho}\frac{\partial p}{\partial x} \tag{2.3b}$$

Where f is the coriolis force, and u and v the zonal and meridional phase speed respectively (Andrews, 2010).

Changing the speed of air is both the cause and effect mechanism of a difference in pressure. Pressure difference is equivalent to a force per unit area. And that is the driving force of the phenomenon *wind*. But to initiate a pressure difference in the atmosphere, we look at the temperature which varies with latitude, longitude and altitude. In hydrostatic balance we can neglect the vertical motion, and assume that the temperature is locally constant with height, and only varying with latitude. We also assume geostrophic

balance and that the perfect gas law holds. Since the pressure is closely dependent on the temperature, and the pressure gradient is the source for wind change, a latitudinal temperature gradient results in vertical gradients of horizontal wind.

To describe the relation between the temperature gradient and wind speed we can establish an equation called the Thermal Wind Equation (TWE). By following the procedure from Andrews (2010) we get, by applying the hydrostatic equilibrium (equation 2.2) on the geostrophic approximation (equation 2.3) and the perfect gas law 2.1:

$$-\frac{g}{R_a T} = \frac{\partial \ln p}{\partial z}$$

If we procede with neglecting the vertical variations in T (hyd. bal.), we can cross-differentiate and get the thermal windshear equations, or Thermal Wind Equation:

$$f\frac{\partial v}{\partial z} \approx \frac{g}{T}\frac{\partial T}{\partial x} \tag{2.4a}$$

$$f\frac{\partial u}{\partial z} \approx -\frac{g}{T}\frac{\partial T}{\partial y} \tag{2.4b}$$

Where u is zonal velocity and v medional velocity. These equations gives us useful relations between horizontal temperature gradients and vertical gradients of the horizontal wind, when both geostrophic balance and hydrostatic balance apply. If the wind shear gradient in the vertical gets too strong it can lead to a baroclinic instability leading to a release of kinetic energy from the moving parcels of air.

In the mesosphere however, when gravity waves breaks, they create *ageostrophic* flow. But since they are filtered by the lower atmosphere, which *is* in geostrophic balance, the sign (if not the magnitude) is correct.

2.3 Wave systems - Origins and behaviour

Different types of waves are prominent in the atmosphere, and the three major classifications of waves are presented here.

2.3.1 Gravity waves

Gravity waves are a wave disturbance where parcels of fluid displaced from hydrostatic equilibrium try to stabilize themselves again with help from gravity and buoyancy force

(the restoring forces). At the earth's surface, the ocean waves are a good example of the gravity waves. Ocean waves created by the wind will eventually come to rest as the wind slows down. This is the result of the gravitational force, or in other words, the buoyancy. The density of the air in the wave trough is lighter than the surrounding water, and therefore rises. While the water in the wave crest has higher density than surrounding air and therefore falls. The waves in the atmosphere behave in a similar way, but unlike the ocean surface, where there is a sharp difference in density below and above the surface, the density falls off continuously in the atmosphere. For an isothermal atmosphere, the density decreases exponentially. Instead we need to look at it like lots of thin layers with densities decreasing with height. When a parcel of air is displaced in the vertical direction, the surrounding parcels of air have densities that are either lower or higher than our parcel. This then leads to the restoring effect like the one we see at the ocean surface. And since we now look at a continuous stack of layers the wave aslo propagate vertically as well as horizontally (Andrews, 2010).

The waves origin can be found several places. They can e.g. be a result of airflow over mountaintops, by convective activity in the troposphere or they can even be generated in the middle atmosphere due to gravity- or planetary-wave breaking (Fritts, 2003). Since the waves generated at the lower atmospheric layers can propagate upwards, they can get a considerable increase of amplitude since the density decreases with height. When interacting with the background winds in different regions of the atmosphere, they can encounter regions of dynamical instability, where they cease to propagate and deposit their energy and momentum locally (Andrews, 2010). For those that continue upwards, the increasing amplitude can cause the temperature perturbation to exceed the adiabatic lapse rate, and the wave 'breaks' and dissipates all its energy into the surroundings (Demissie, 2013).

2.3.2 Tidal waves

During the day, the Sun radiatively heats one side of the earth. In the stratopause, the concentration of short wavelength absorbing gases, ecspecially ozone, O_3, is considerably higher than at lower altitudes. So the heating rate reaches a peak at around 50km. The equatorial region gets more radiation per unit area because of the positioning relative to the sun, thus the heating due to absorption is stronger here. This localized heating and expansion of the column of air at the sub-polar point leads to pressure gradients in both latitude and longitude and a forcing of the wind (as explained earlier). During daytime, the heating due to radiation steadily increases from zero before sunrise to its maximum

at zenith, and decreases until it reaches zero at sunset. Since the heating rate is not a pure sinusoid as it is zero during night time, we must use Fourier series to describe the heating mathematically.

$$J_\lambda(t) = \sum_n A_n(z, \theta, \lambda) \cos\left(\frac{n2\pi t}{24} + \phi_n(z, \theta)\right) \tag{2.5}$$

Here $A_n(z, \theta, \lambda)$ is the amplitude of the different wave components numbered n. The different values of n separates the differenct components of the heating, and are called the atmospheric tidal waves. Each one with its own name: $(n = 1)$ is called the diurnal, $(n = 2)$ the semidiurnal, $(n = 3)$ the terdiurnal and so on. We can describe two types of atmospheric tidal waves, the migrating and non-migrating waves. The waves following the Sun around the Earth are migrating. The non-migrating waves are forced at a single point triggered by the heating when the Sun passes by. For example, in the tropics the heating lead to generation of thunderstorms in the warm seas of the Asian area. They create many gravity waves that propagate up into the mesosphere and cause local acceleration when they break. After the Sun passes and the area cools down, the convective activity subsides and the forcing stops. However, in the mesosphere the migrating waves are the dominant ones (Salby, 1996).

Hibbins et al. (2007) studied the climatology of the tides, and showed that in high latitudes the diurnal tide is weak during the summer months, while the semi-diurnal tide is strong. As with the gravity wave, a vertically propagating tidal wave will eventually reach a point where it will break, redistributing energy into the surroundings. This energy can be resonantly absorbed by sub-harmonic wave modes, for example the 2-day wave (Walterscheid and Vincent, 1996).

2.3.3 Planetary Waves

Planetary waves, or Rossby waves, are waves with horizontal scales of thousands of kilometres and with periods of several days (Andrews, 2010). They exist in simple background flows were they propagate in a westward direction relative to the zonal wind. They can be excited by large-scale diabatic heating in the Troposphere due to land-sea temperature differences and variations in the orography. When doing so, a restoring force comes into play (as with any wave). In this case the restoring force is the variation of the Coriolis force with latitude.

If we first assume horizontal motion only, one can look at different features with the wave at each level. We start by assuming a barotropic atmosphere with only horizontal flow,

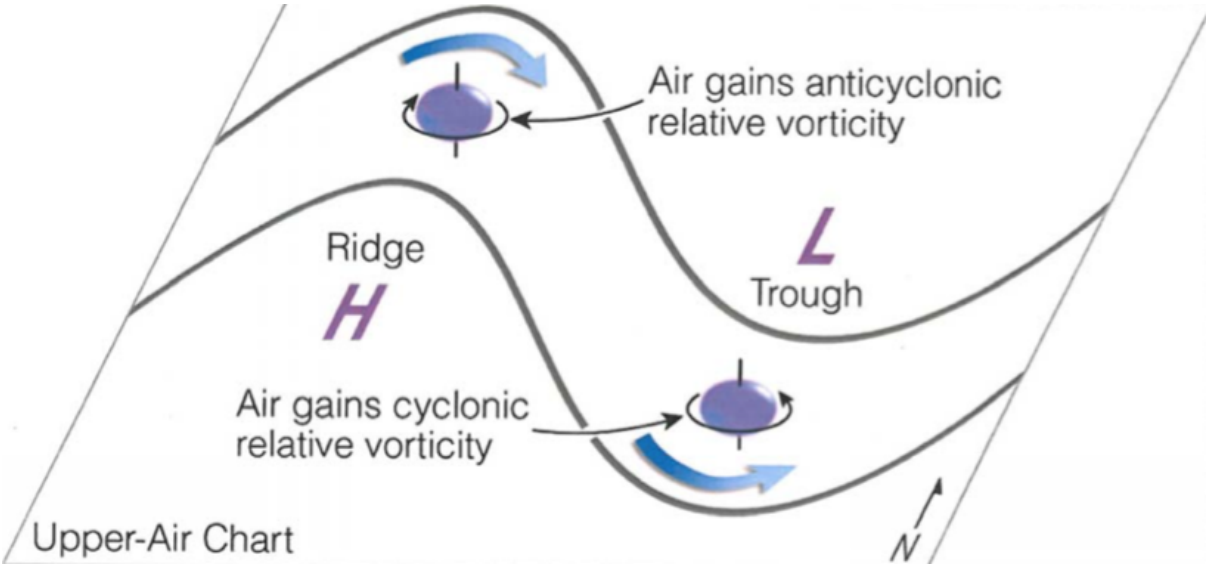

Figure 2.1: The conservation of absolute vorticity, leading to a westward propagating wave. Courtesy of Steve LaDochy, California state University.

and instead of using a spherical geometry, we use cartesian geometry which is known as the ***β*-plane approximation**. In a barotropic, non-divergent fluid, the Coriolis force is a result of the conservation of absolute vorticity. This conservation of absolute vorticity can be expressed as:

$$\frac{d\eta}{dt} = \frac{d(\xi + f)}{dt} \tag{2.6}$$

where η is the absolute or total vorticity, ξ the relative vorticity associated with the angular momentum of a fluid parcel about its centre of mass, and f the planetary vorticity associated with the motion of the centre of mass of the parcel around the Earth's rotational axis. In our approximation we can describe the Coriolis parameter with linear variability in meridional direction, $f \approx f_0 + \beta y$, where $f_0 = 2\Omega \sin \Phi$, where Ω is the angular speed of the Earth's rotation and Φ is latitude. The meridional gradient, β, in this equation is called the Rossby parameter, and is expressed as:

$$\beta = \frac{2\Omega \cos \phi}{a} \tag{2.7}$$

where a is the Earth's mean radius, and ϕ the latitude. This implies the following: If you displace a parcel of air in a northward direction (being in the northern hemisphere) and think of equation (2.6) the **planetary vorticity** f of the parcel is increased as it moves closer to the center of the Earth's rotational axis. To conserve its **absolute vorticity**, its **relative vorticity** must decrease. Thus the parcel increases its spin in clockwise direction (reduces cyclonic relative vorticity). Equivalently it increases its relative vorticity when

displaced in the southward direction, gaining spin in the anti-clockwise direction (gains cyclonic vorticity).

To examine the wave propagation one must think of this parcel to be a cylindrical blob of air. The northward displaced parcel of air, spinning clockwise, also interacts with its closest neighboors in the west (and east), displacing *them* northward (and southward), causing yet another vorticity-change. This effectively creates a horizontal, westward propagating wave motion.

As well as the horizontal motion generated by this mechanism, the decrease (increase) in relative vorticity when travelling northward (southward) makes the cylindrical parcel shrink in the vertical plane due to this reduction. Southward it would strech out in the vertical direction. This process leads to vertical as well as horizontal propagation.

The planetary waves have a phase speed c in the horizontal plane (defined to be positive in eastward direction) which is of the same order as the mean zonal wind. This makes them easily affected by interactions with the wind flow. This interaction or dependency is described by the dispersion relation for Rossby Waves:

$$c \equiv \frac{\omega}{k} = U - \frac{\beta}{k^2 + l^2 + f_0^2 m^2 / N_B} \tag{2.8}$$

where U is the mean zonal wind flow, ω is the angular velocity and k and l the horizontal, and m the vertical, -wavenumbers. When we look at pure horizontal motion, $m = 0$, equation (2.8) reduces to

$$c = U - \frac{\beta}{k^2 + l^2} \tag{2.9}$$

With the Rossby parameter always being positive, the second term is always positive. Thus the phase speed must be $c < U$ and the relation $0 < U - c$ must always hold. This means that the waves with its crests and troughs will always move *westward* relative to the backgroud flow, and the phase speed relative to the flow must be negative. PWs with slow phase speed, will be swept eastward by the background flow (but still: it is westward propagating relative to the flow). The faster waves can maintain its westward propagation.

From equation (2.9) the phase speed of a wave with fixed frequency is greatly dependent on the wave's wavenumber. With higher wavenumbers, or in other words: shorter wavelengths ($c \propto \frac{1}{k} \propto \lambda$), the speed of the wave slows. With increased wavelength, its phase speed grows (westward direction). A wave like the QTDW, consisting of several modes, is strongly **dispersive**. Different components of a initial disturbance will break up (dis-

perse) in time, since the different wavelength components propagate away at different speeds (Andrews, 2010).

There is however a limit for the PW to be able to propagate, as established by Charney and Drazin (1962), called the critical velocity U_c, and this is expressed as

$$0 < U - c < U_c \tag{2.10}$$

where U_c is defined as

$$U_c = \frac{\beta}{\left[(k^2 + l^2) + \dfrac{f^2}{4H^2N^2}\right]}$$

Here N is the buoyancy or Brunt-Vaisälä frequency and H is the scale height. This means that the PW propagate only when the zonal wind is eastward ($0 < U$) and not too strong ($U < U_c$). A wave encountering a layer with zonal wind stronger than U_c, is slowed down and absorbed there. Since the the critical limit increases with longer wavelengths, the propagation of larger scale waves is allowed at a wider range of background mean wind flow, while the smaller scale waves is dependent on a more narrow range of background flow.

An observer on the ground, sees the waves *observed* frequency, and not the frequency it has relative to the background flow. This observed frequency, ν_o can be described as

$$\nu_o = \nu_I + k\overline{U}$$

where $\overline{U}$ is the mean eastward wind, $k = s/a$ and ν_I the *intrinsic* frequency. The eigenfrequencies retrieved from Laplace's tidal equation are calculated with respect to the frame of reference, namely the moving background flow, and will be constant with respect to the flow, but Doppler shifted relative to the ground. If the mean wind blows eastward (as it does during winter), we expect the atmospheric manifestations of the free Rossby modes to in general be at longer periods since:

$$T_{obs} = \frac{2\pi}{\left|\nu_I + k\overline{U}\right|}$$

The Quasi Two-Day Wave

The following secction is based on the comprehensive articles from Baumgaertner et al. (2008) and Tunbridge and Mitchell (2009). The wave is called the "Quasi Two-Day Wave"

(QTDW) because the wave's period actually varies with several hours, with periods up to 2.2 days and down to 1.7 days.

The reason for this variability comes from the fact that there are several solutions of Laplace's tidal equation that lie close to the 2-day period which all varies in amplitude. The closest component, wavenumber W3, gives the mixed Rossby-gravity wave mode $(3, 0)$ (Salby, 1981), which has a period of 2 days. W4 lies close with a period of 1.7 days. These two are the most prominent but W2 also is reported to be significant in polar regions (Nozawa et al., 2003). With different wavenumbers, the different modes will have different transmission coefficients upwards through the atmosphere, resulting in a high variability of the QTDW's amplitude, as well as the varying period.

A strong stratospheric jet (which also would absorb most waves propagating through it, especially if the jet is westward like in summer) can cause baroclinic instability above itself. While most wave modes originated in lower altitudes would be absorbed in this region, the W3-mode is easily generated in the mesosphere by this instability (Plumb, 1982; Baumgaertner et al., 2008). The wave amplitude can become large when its free period QTDW becomes very close to a sub-harmonic of the tides (i.e. 48 hrs) as it can draw energy from the tidal oscillations.

2.4 Spectral analysis

To track frequencies and amplitudes of the different wavecomponents in the data, two algorithms where used to produce a frequencyspectrum, the Fast Fourier Transform (FFT) and the Maximum Entropy Method (MEM). Applied to a discrete set of data, the FFT is in principle finding the set of sine waves that will reproduce the data set in the best possible way.

When applied to a finite set of data, the sharp transitions at the end of the set causes the FFT to produce many high-frequency components to best reproduce the cut-off. To reduce that effect, a Hamming-window is applied to the data. The Hamming window is chosen amongst others because of its strong effect on the sidelobes of each frequencypeak in the spectrum, in fact the first sidelobe is reduced to a amplitude of 0.007 times the amplitude of the peak. However, the peak will be wider (Press et al., 1992).

The FFT calculates only $\frac{N}{2}$ frequencies between 0 and the Nyquist-frequency ($\frac{1}{2F_s}$). If the number of datapoints N is low, then the frequency sampling gets low. By adding zeros to the data set, N is raised, and the frequency sampling is improved (Press et al., 1992).

Another algorithm for transforming datasets over to the frequency domain is by the Maximum Entropy Method (MEM) (Press et al., 1992).

$$\frac{a_0}{\left|1 + \sum_{k=1}^{M} a_k z^k\right|^2} \approx \sum_{j=-M}^{M} \phi_j z^j \tag{2.11}$$

This method takes in use a different approach, which does not fit sinusoids to the data to define its frequency components. Instead, one specifies a number of autocorrelation coefficients (AC). These define the poles and zeroes of a digital filter that when applied to Gaussian white noise, reproduces the time-domain data in the sample interval while maintaining Gaussian white noise at all times. If the calculation has only one AC, one would find a peak at the most prominent, or "important" frequency which best describes the original signal. Adding more AC's, reveals a more detailed frequency spectrum. With many AC's additional frequency elements are added to fit the random noise present in the data. A general recommandation is to have at least a few times the number of sharp spectral features that one desires to fit (Press et al., 1992). A higher number means sharper peaks and better resolution, but it is also recommended to stay below half the number of datapoints to watch out for the noise peaks.

The comparison between the FFT and the MEM can be visualized by creating a signal with added noise and run the algorithms to view their strenghts. The following test uses a signal consisting of sine waves at 0.2 cpd, 0.5 cpd and 1 cpd with amplitudes of 5, 1 and 5 respectively. Gaussian white noise is then added with a deviation of 1. The FFT and MEM is applied to the data using a 6-day range.

As figure 2.2 indicates, the frequency spectrum by FFT clearly extracts the 5-day wave and the 1-day wave, but the 2-day peak seems to be shifted 0.1 cpd to 0.4 or 0.6 cpd. This is du to the fact that the FFT algorithm get into difficulties when the period of the wave in the signal is near the length of the data set. However, the amplitudes given from the FFT-spectrum are more correct. To find the frequency peaks the MEM is far better in this case. Figure (2.2c) shows the MEM with three different numbers of ACs (30, 60 and 90). Through several tests of the number of AC, 60 gives us the best definitions of the peaks (the 2-day (0.5 cpd) wave is generally found at 0.4980 cpd), as too high number of AC occasionally can generate noise peaks within our interval, and too low number of AC is unable to resolve the 2-day from the other components nearby.

So by combining the frequency from MEM, within the range of 0.3 and 0.7 cpd, with the corresponding amplitude from the FFT, we get a good track of how the QTDW activity is.

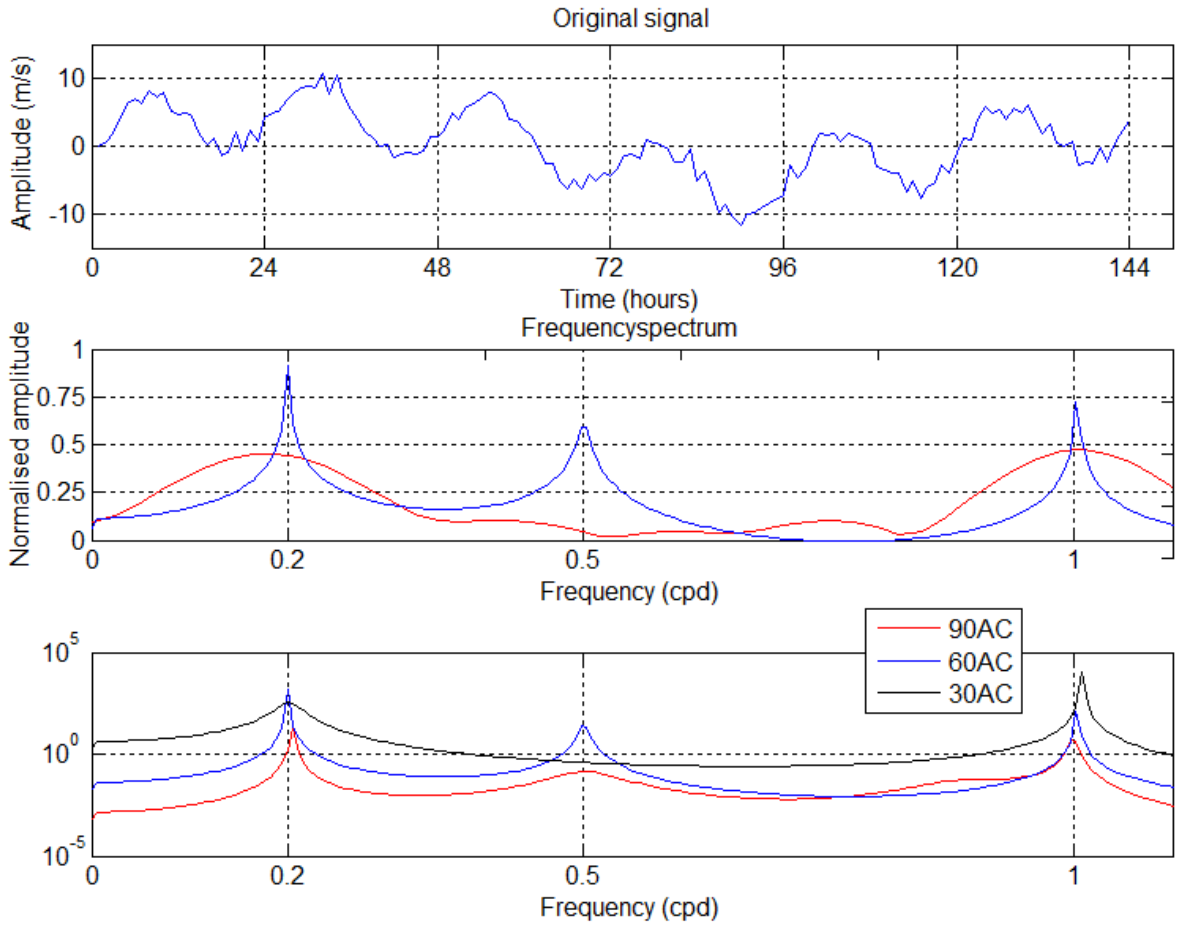

Figure 2.2: (top) Original signal consisting of sine waves with periods of 5 days (0.2 cpd), 2 days (0.5 cpd), 1 day (1 cpd) and Gaussian white noise. (middle) The frequencyspectrum as computed by FFT (red) and MEM (blue). (bottom) MEM frequency spectrum using different numbers of Autocorrelation Coefficients (AC).

Chapter 3

The SKiYMET radar

During a 24-hour period many sporadic meteors (i.e. those not associated with meteor showers) enter the Earth's atmosphere. As the density increases, the friction forces on these small particles increase such that they burn up, leaving a trail of ionized particles. These trails can be observed and tracked by radars as they are advected by the local wind field, giving us valuable information of the neutral wind velocity at the altitude of the trial. For this thesis the main focus will be the wind speed and wind direction observed by the meteor radar positioned at Dragvoll, Trondheim ($63°N, 10°E$).

3.1 How it works

In order to study the winds in the mesosphere we use a radar technique as described by Hocking et al. (2001). The SKiYMET radar system searches for meteor echoes in the mesosphere by transmitting electromagnetic pulses towards the sky where the ionized particle trail reflects some of these pulses. The recieving antennas back at the ground register the reflected signals. Because there are 5 recieving antennas, the system is able to triangulate the meteor trails in all 3 dimensions, and observe how the wind moves it. Thus it is able to read the background wind at the location of the trail. Since the recievers count over 10000 such meteor trails each day, we can calculate the winds on an hourly basis with a vertical resolution of $\sim$ 2km between 81 and 98km

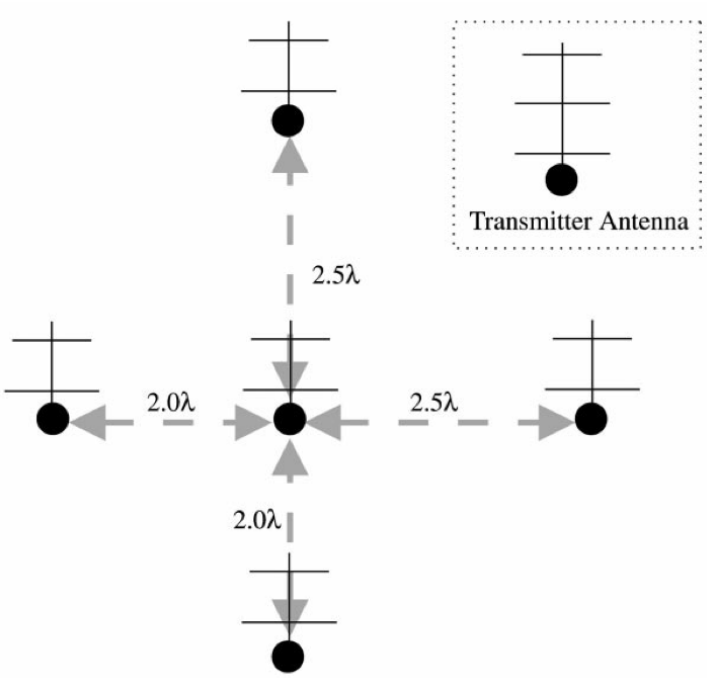

Figure 3.1: The SKiYMET radar set up as of Hocking et al. (2001)

Chapter 4

Analysis and results

4.1 Data processing in MatLab

The SKiYMET radar measures and stores data in easily accessible files called HWD-files. In order to getting access these files, all the tools for processing and plotting the data was developed completely in MatLab 8.0.0 (R2012b). The data being analyzed range from the beginning of October 2012 to September 2013. There were some some downtimes of the SKiYMET radar which are viewed in plots as white fields.

In this thesis only the zonal wind data are extracted. The data are in a format of hourly samples of the wind amplitude at all six heights (range 81-98 km). A brief explanation of how the program procedure operates is as follows: The data are taken in segments of 6 days for the spectral analysis processing. After the first segment, the 6-day window is shifted by one day for the next segment to be analysed. In this way, the amplitude and frequency can be studied as a function of time. The two different algorithms, the Fast Fourier Transform (FFT) and Maximum Entropy (ME), are then applied to each of these segments to extract the frequency-components and their corresponding amplitudes. Since Baumgaertner et al. (2008) and others report a burst-like behaviour from the QTDW and a slightly changing period depending on time of year and location the segment is set to 6 days to know that the FFT has a long enough data segment to resolve the QTDW peak. MEM is used primarily to localise the frequency accurately, and based on these frequencies the amplitude is extracted from the FFT.

There are several days of missing data during the dataset due to downtime of the radar. These are viewed as white sections in the plots. To be able to work around these with the FFT and MEM algorithms, a linear interpolarization was used to produce the spectrum,

and the days of missing data were afterwards marked with white regions so that no wave components are reported within the interpolated regions.

4.2 Seasonal occurrence

Figure 4.1a and 4.1b shows the frequency spectrum of the entire range of available data at the highest altitude (98km). To save space, the equivalent plots for the other altitudes are given in appendix A. The two spectra show very similar structures, although the frequency peaks in the MEM-spectrum are more sharper defined.

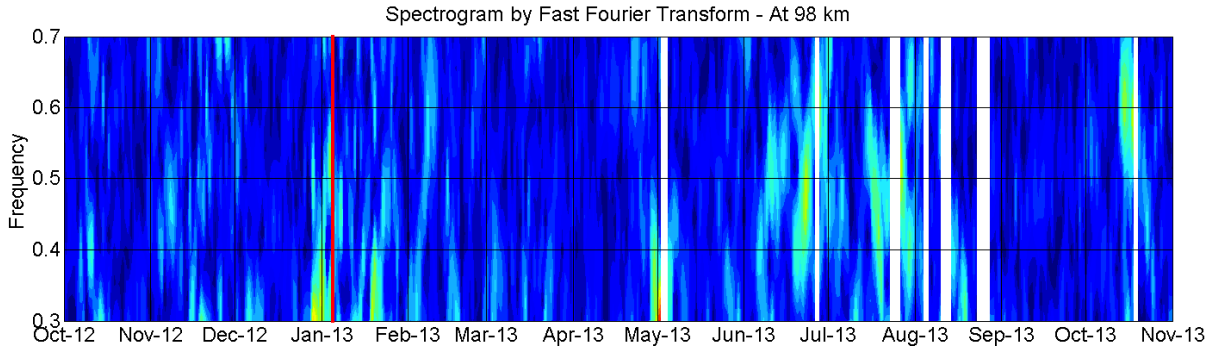

(a)

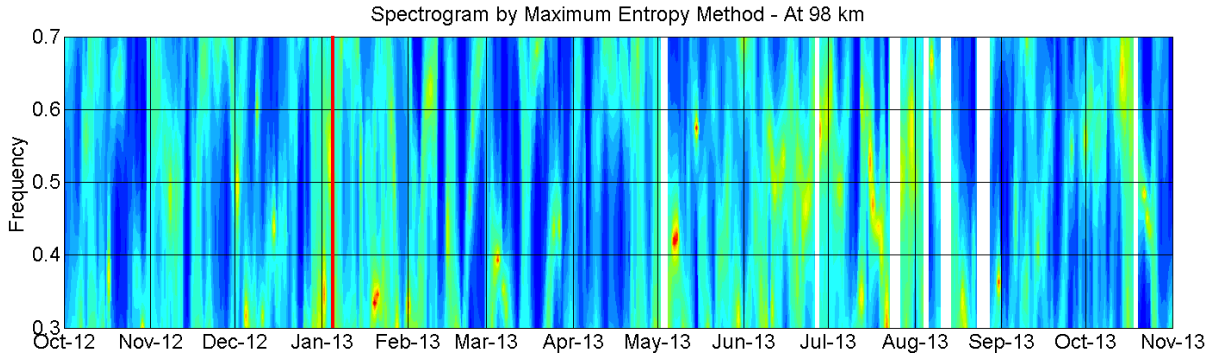

(b)

Figure 4.1: Frequencyspectrum as computed by (a) FFT an (b) MEM. White fields are days of downtime by the radar and the red vertical line on 6th of january is the SSW event. Solstice is at mid-june.

As expected there is almost no wave activity around the equinoxes. In wintertime, one can see the bursty nature of all wavecomponents near the 2-day period (or 0.5cpd). This feature of the QTDW is consistent with earlier studies (i.e. Baumgaertner et al., 2008; Tunbridge and Mitchell, 2009; Nozawa et al., 2003). The different wave-modes have different transmission coefficients through the stratospheric jet due to their wavelength

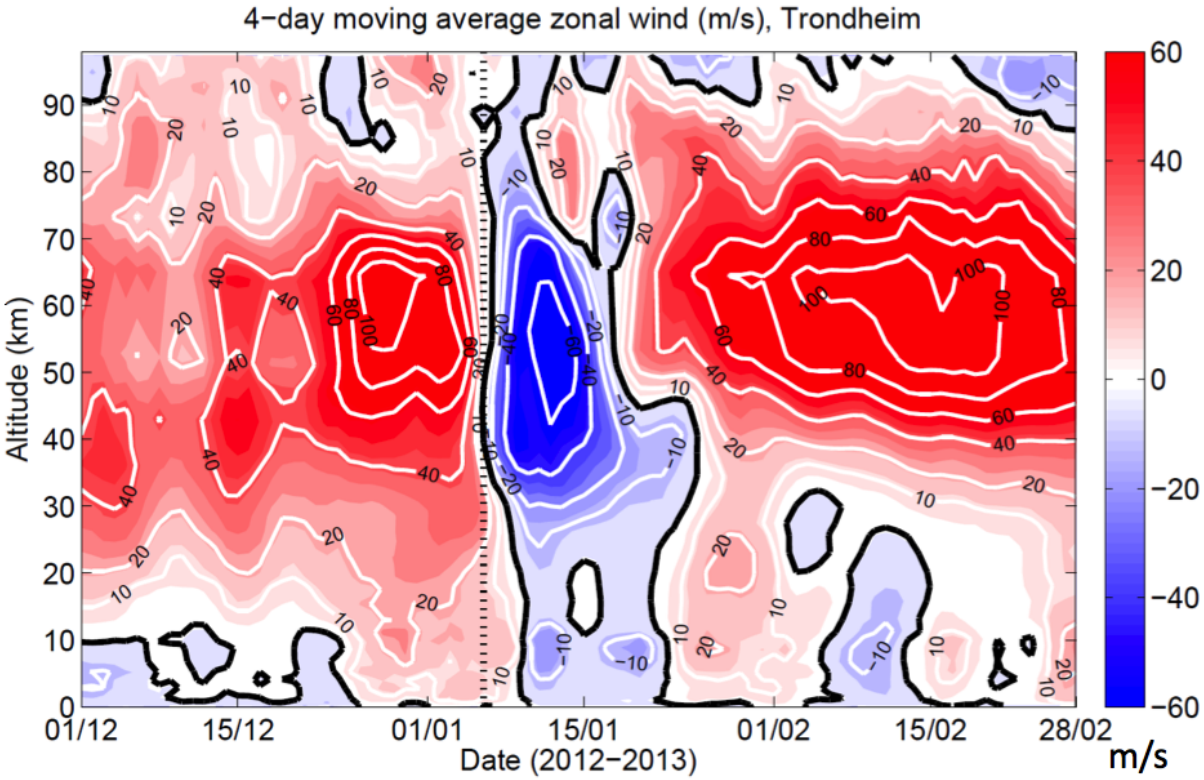

Figure 4.2: 4-day moving average zonal wind above Trondheim. Notice the strong wind shear at around 90km from mid january. Courtesy of Rosemarie de Wit, Norwegian University of Technology and Science.

differences, hence the different modes appear somewhat sporadically in the mesosphere at different times.

There is however in January a small enhancement of amplitude at several different frequencies between 0.3 and 0.7 cpd with no enhancement of the W3 component over the others. In January a breakdown of the polar jets took place in an event known as a Sudden Stratospheric Warming (SSW, marked with a red line in figure 4.1a and 4.1b). During the event, the winds in the Stratosphere are very weak and, for a short time period, westward (figure 4.3). This means that the critical limit for propagation of a planetary wave is almost removed. Thus we see an increase of QTDW-activity during the SSW at all frequencies. Due to the strong warming in the stratosphere, and later during the recovery phase, there are strong shears in the vertical profile of temperature (as seen in figure 4.2) since the mesosphere above is very cold. This instability can force the W3-component in situ and therefore account for its intensification during and after the SSW.

Through the summertime, the QTDW-activity increases significantly at solstice through mid-august. Here there is a consistently high amplitude and relatively stable period, with

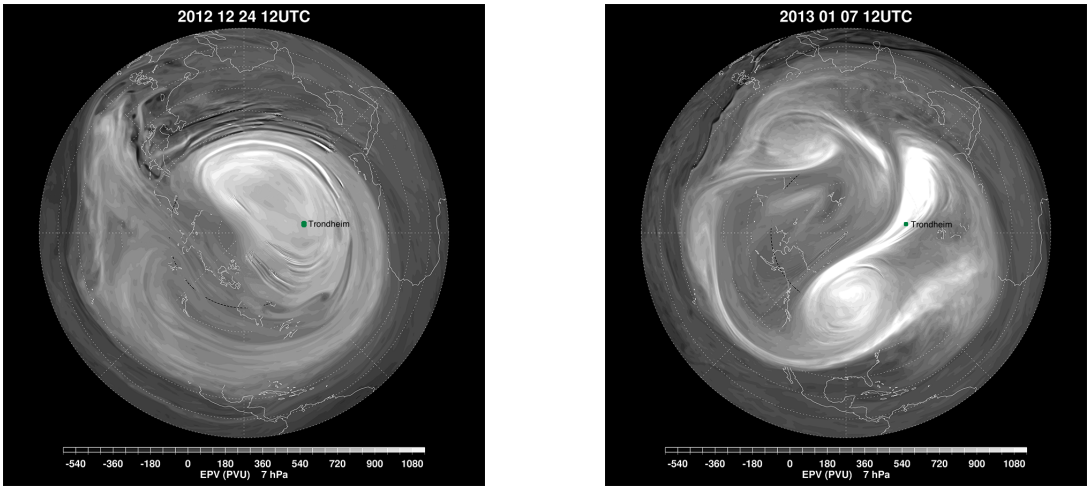

(a) December 24 (b) January 7

Figure 4.3: The breakdown of the wintertime stratospheric vortex above Arctic 2013 near 35km. Note that our radarlocation (marked with a green dot) at Trondheim ($63°N$) is measuring only what happens above that location (Coy and Pawson, 2013)

frequencies closer to the 2-day period being amplified. The occurence is stable with time, being prominent through several days or weeks. These features are also the known characteristics from earlier studies (i.e. Baumgaertner et al., 2008; Tunbridge and Mitchell, 2009). The consistency of the wave during summer indicates an in situ forcing of the wave. The westward wind in the Stratosphere effectively blocks vertically propagating waves, removing the unstable propagation from below. But the strong temperature gradient created due to the heating (hot stratosphere, very cold mesosphere) above the jet leads to an instability that forces planetary waves.

As well as the instability forcing of the wave, the semi-diurnal tide dissipating in the mesosphere may also force the sub-harmonic W3 wave component at higher altitudes. To examine that, the following section will focus on the altitude behaviour of the QTDW.

4.2.1 Amplitude vs frequency

Figure 4.4 shows the strongest amplitude component in the frequency range 0.3-0.7 cpd extracted from the spectra (figure 4.1a and 4.1b) each day between the beginning of October 2012 and November 2013. The plots are consistent with the spectrum showing a relatively sporadic amplification of the different frequencies, with no consistently strong maximum at any wave-component. One can however see some enhancement of frequencies near 0.5 cpd at 98km and slightly weaker at 94km. The frequencies around 0.35 cpd and 0.65 cpd experiences also a small enhancement at 98km. Below 94km, there is an even

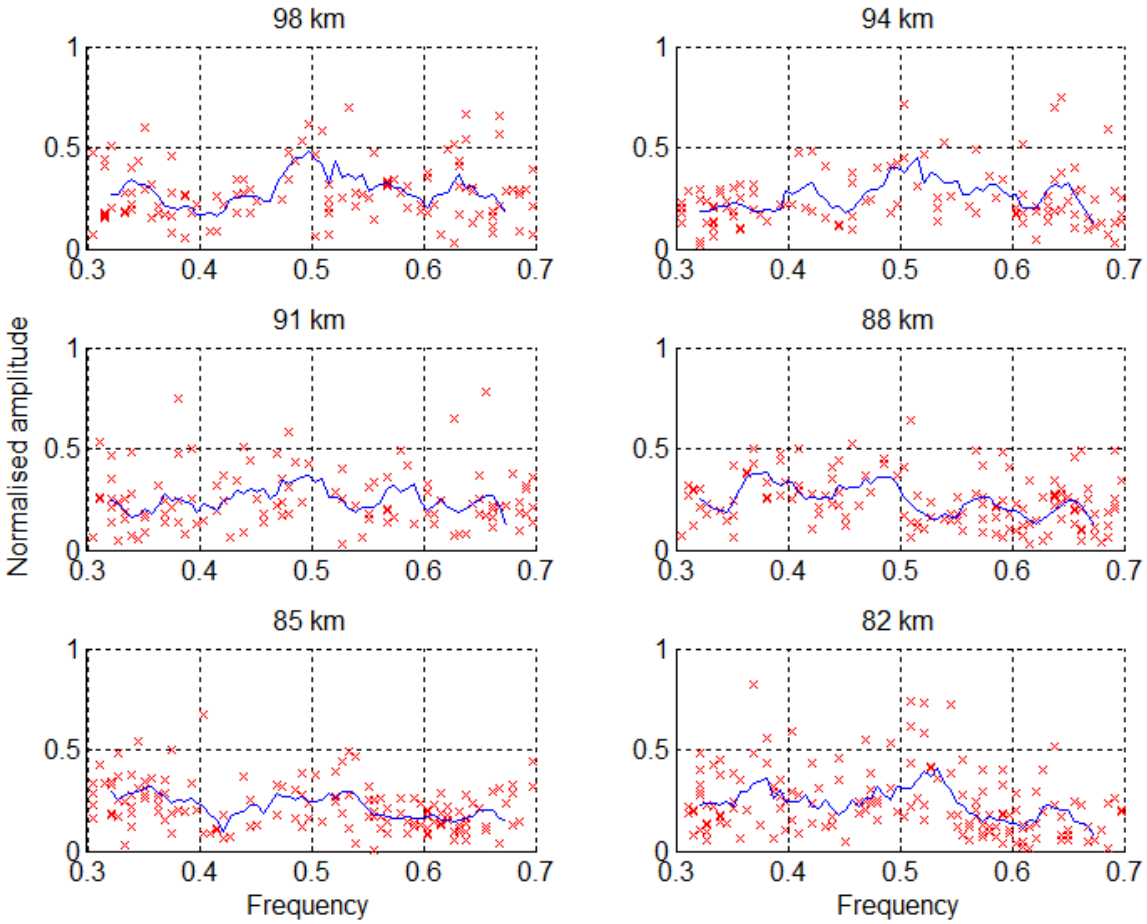

Figure 4.4: Amplitude as a function of frequency, extracted out of data from october through mars. Moving average of amplitude at frequency binwidth of 0.006cdp.

distribution with frequencies. However, a tendency in the distribution at 82km shows that the 0.5 cpd frequencies are slightly enhanced. But since the data points are scattered as widely as they are, no clear cause and effect mechanism is being proposed here.

The high altitude enhancement can be connected to the recovery phase of the stratospheric warming. The enhanced QTDW activity appears to be predominantly at around the 2-day period, and likely associated with the W3 component being generated in the strong shears at high altitudes during the SSW recovery.

Through summer between April 2013 and October 2013 (figure 4.5) there is a similar enhancement of the above frequencies, but the W3 component is amplified much stronger. There is also a weak enhancement of frequencies near 0.35 cpd, and to a certain extent the ones near 0.65 cpd, but these enhancements are not found below 94km and the 2-day component seems to be the only significant one. As the semi-diurnal tide being strong during summer, and that the strong enhancement is primarily happening at the highest

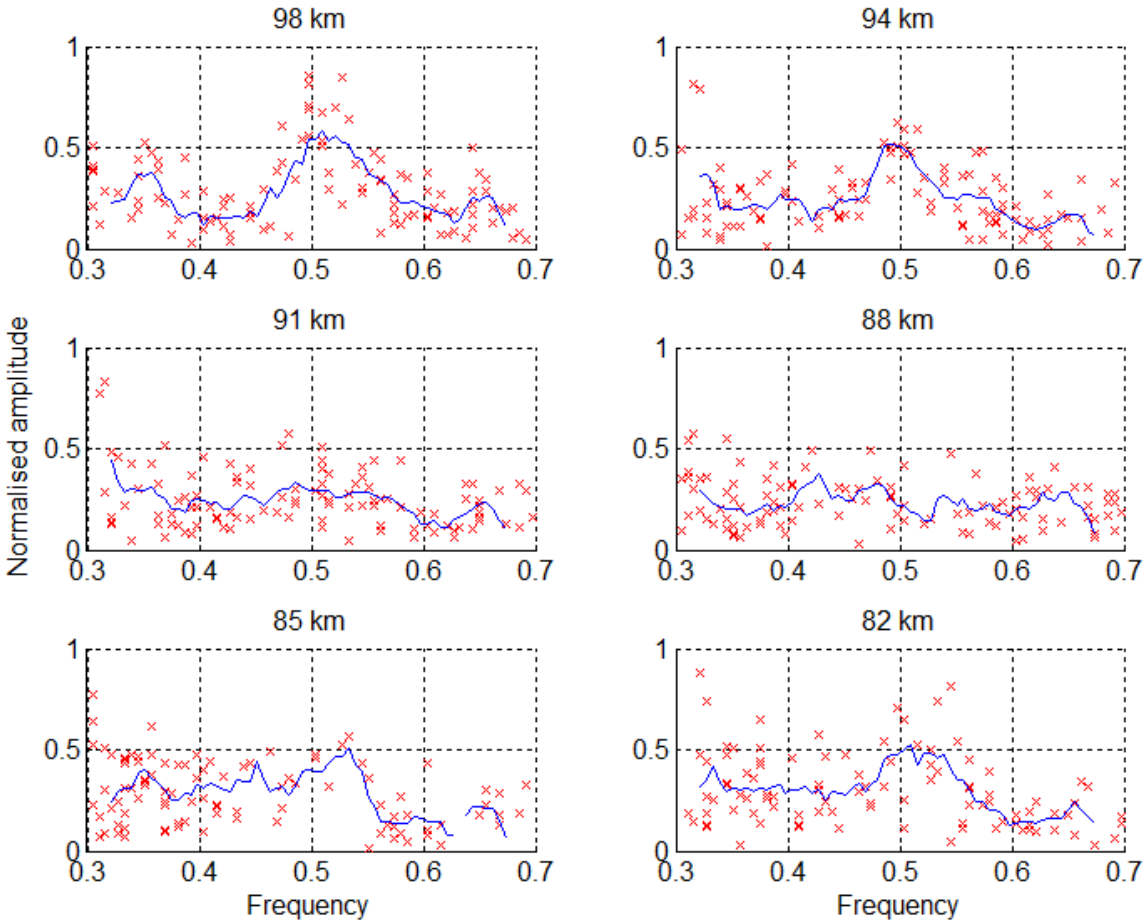

Figure 4.5: Amplitude as a function of frequency, extracted out of data from april through september. Moving average of amplitude at frequency binwidth of 0.006cpd.

altitudes, is consistent with the coupling to the tide, which begins to dissipate its energy at the higher altitudes. There is also a weak enhancement of the 2-day component at 82km, just above the zonal wind jet. As this plot only show us the overall relation between the amplitude and frequency at a given time range, we need a plot that can show us at which time of the year, and at which altitudes the period of the QTDW stabilizes near 2 days.

4.2.2 Occurrence as a function of height and time

To examine where and when the QTDW amplitude stabilizes at the W3 period of 48 hours, the frequency of the maximum amplitude as a function of altitude and time is plotted. Figure 4.6 shows the strongest frequency at all altitudes and times between 0.3 and 0.7cpd. The color scale goes from black to green as the frequency approaches 0.5cpd from both above and below 0.5cpd.

In wintertime (figure 4.6a) we can see that if the W3-component shows up, it is in general found at all altitudes and only prominent for a short time. This is again confirming the variable transmission coefficients of the wave modes. After the SSW event however (late january), the W3-component is amplified between 90 and 98 kilometer. From figure 4.2 one can see that when the vertical wind shear is particulary strong at around 90km from late january until february it also is a source for instability forcing.

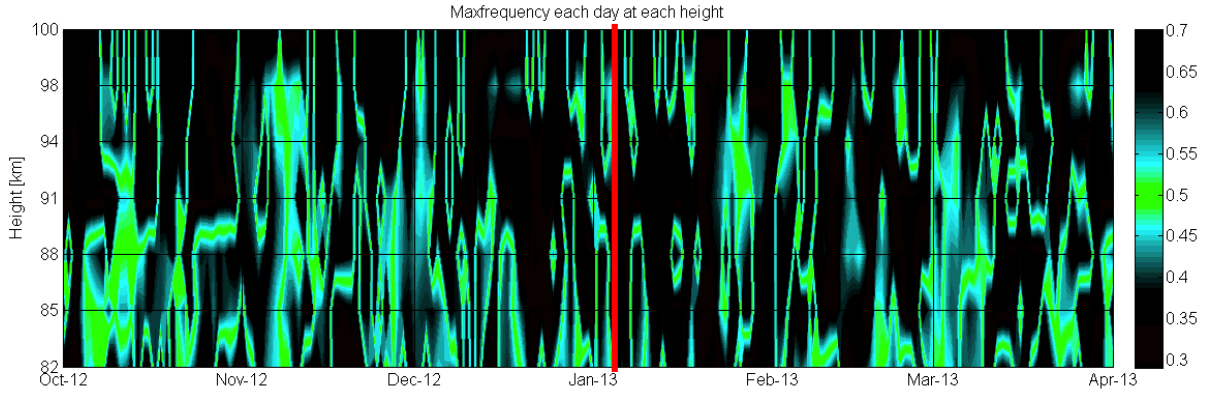

(a)

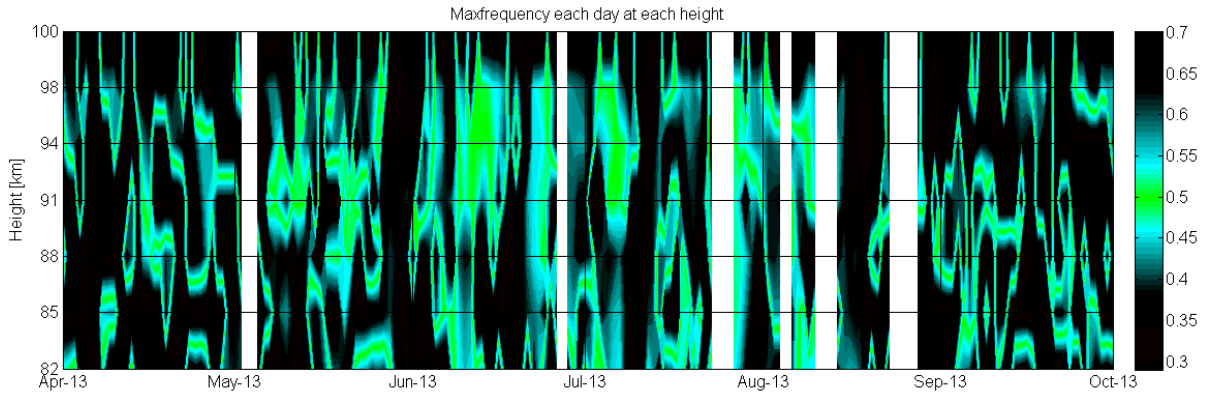

(b)

Figure 4.6: Occurrence of near 0.5 cpd frequencies, centered around the W3 mode, during (a) winter and (b) summer. The red line indicates the SSW event.

Around summer solstice (figure 4.6b) the prominence of components near 2-day (W3 and W4) is significantly more consistent, although not over the entire altitude range. The wave is phase locked at 2 days from 91 to 98 km between mid-june (solstice) to mid-august with few exceptions. The wave is less stable at low altitudes, indicating the amplification of QTDW to occur in situ at higher altitudes. The strong wind and temperatures shears during summer seem to force the W3 mode. However the increasing amplitude at the highest altitudes also indicates an enhancement due to the breaking of the semi-diurnal tidal wave, pumping the 2-day component W3.

Chapter 5

Conclusion and further work

Retrieved data from the SKiYMET-radar at Dragvoll, Trondheim ($63°N, 10°E$) were examined to observe the amplitude and frequency behaviour of the QTDW during both winter and summer (figure 4.1). A clear enhancement of the wave after summer solstice indicates that shear instability indeed plays a role in the generation of the QTDW as suggested by Plumb (1982) and Baumgaertner et al. (2008). In winter the solstice was disturbed with an SSW event, weakening the winds and thus leading to an enhanced planetary wave activity at all frequencies within the range investigated. However, the strong wind shear near 90km associated with the recovery of the winter conditions seems to result in the in-situ generation of the QTDW in the period after the event. In summer, there is a more clear-cut enhancement of the QTDW that seems to be phase locked at the W3 period, or 0.5 cpd (2-day period).

How and where the amplification of the different wave-modes took place were investigated through relating the amplitude to the frequency at all altitudes. The figures for both winter (figure 4.4) and summer (figure 4.5) indicates similar features as obtained previously. However, the summer plot emphasises the strong enhancement of the 2-day component to occur at 94 and 98 km, indicating an in situ generation of the W3 component by tidal forcing mechanism.

Finally, the occurence of well defined near-0.5cpd wave modes as a function of both altitude and time were examined. The consistency in presence of the W3 component from summer solstice through mid august with few exceptions strongly indicates that the wave must be generated in situ. The summer stratospheric jet being hot and westward, effectively blocking vertically propagating planetary waves and reducing the bursty behaviour, are strong indications of the baroclinic instability-forcing of the wave. And since the wave clearly maximises at the highest altitudes, especially the W3-component,

the semi-diurnal tide dissipation is most likely to be a strong forcing mechanism of this component.

By the different steps of analysis the results of this thesis indicates that the QTDW in summertime indeed is a result of both baroclinic instability and a pumping mechanism of the dissipating semi-diurnal tide as expected. In wintertime, its amplification is dominated by the variable transmission coefficients of the different wave-modes, however during and after the SSW event the amplification at higher altitudes is more consistent suggesting the instability causing the forcing of the W3 component.

For future work on the QTDW and the semi-diurnal dissipation it would be interesting to look at how the tidal amplitudes varies with altitude during summer to see if they grow as expected ($A(z) = \exp(z/2H)$), or if they dissipate their energy into the surroundings. This would give us important answers to if the tidal waves indeed are the forcing mechanism for the high altitude QTDW.

Appendix A

Figures

The following figures A.1-6 are the spectra computed by the (a) FFT algorithm and (b) MEM algorithm. A red line on 6th of January shows when the SSW occurred.

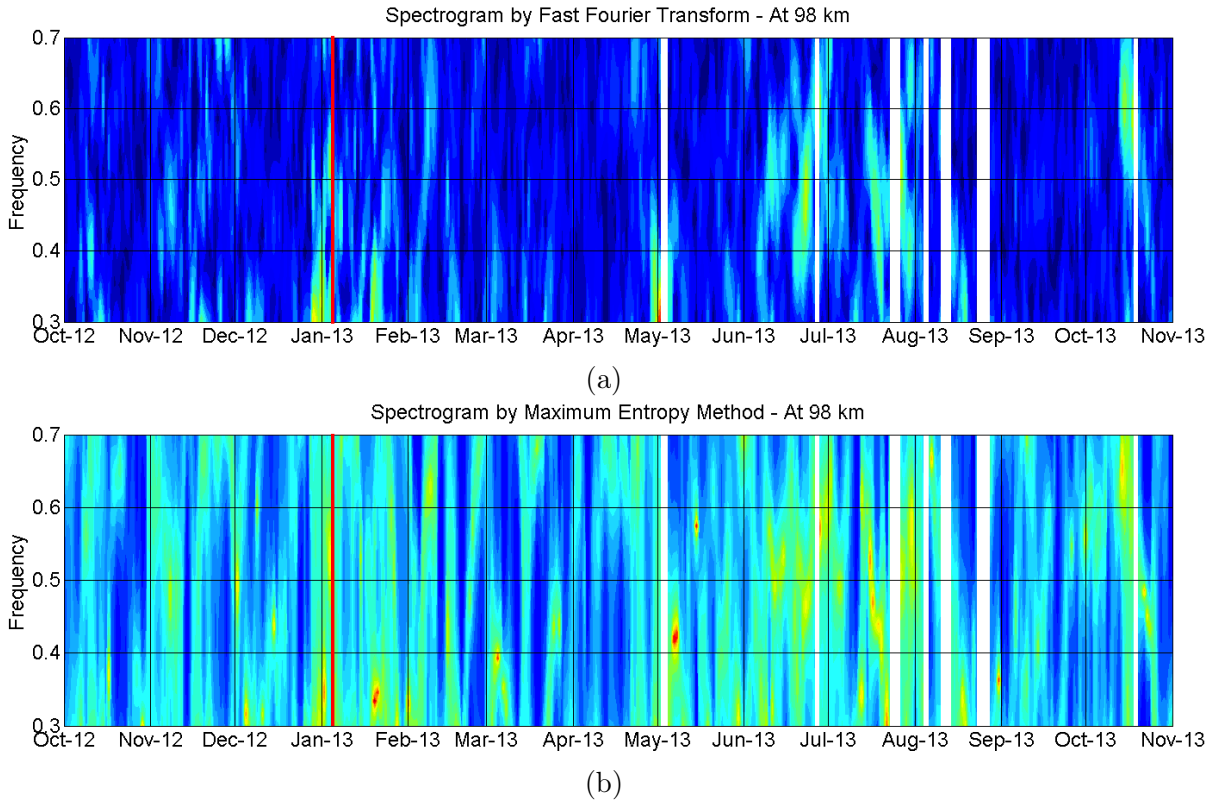

(a)

(b)

Figure A.1: Frequencyspectrum by (a) FFT and (b) MEM at 98 km

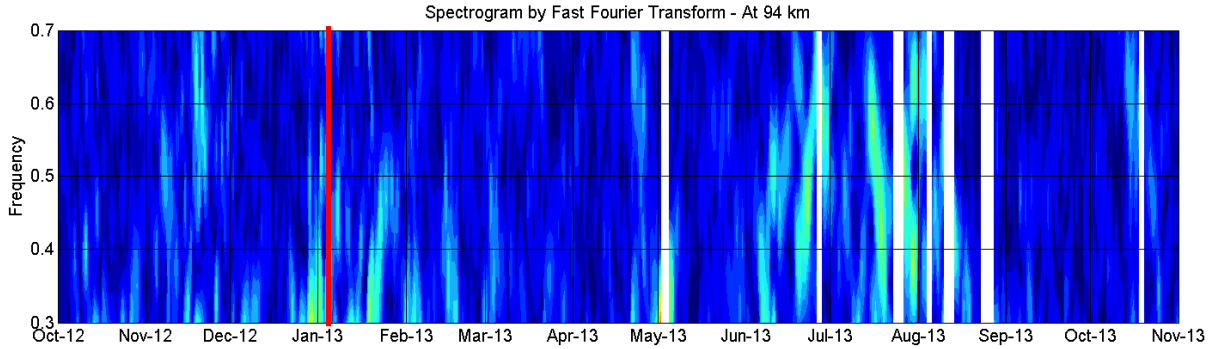

(a)

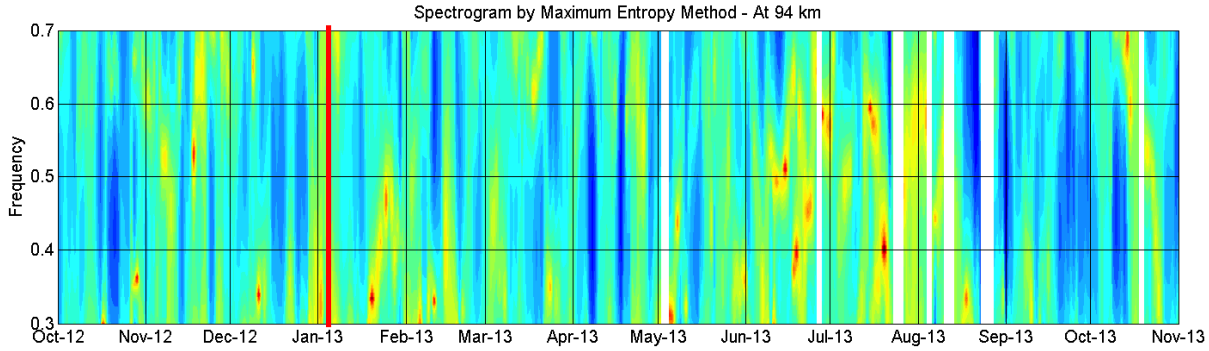

(b) Frequencyspectrum by (a) FFT and (b) MEM at 94 km

Figure A.2: Frequencyspectrum by (a) FFT and (b) MEM at 94 km

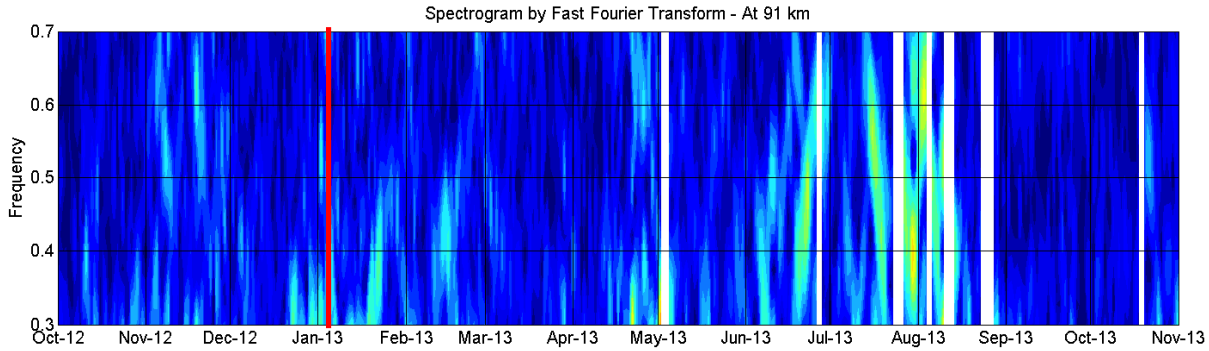

(a)

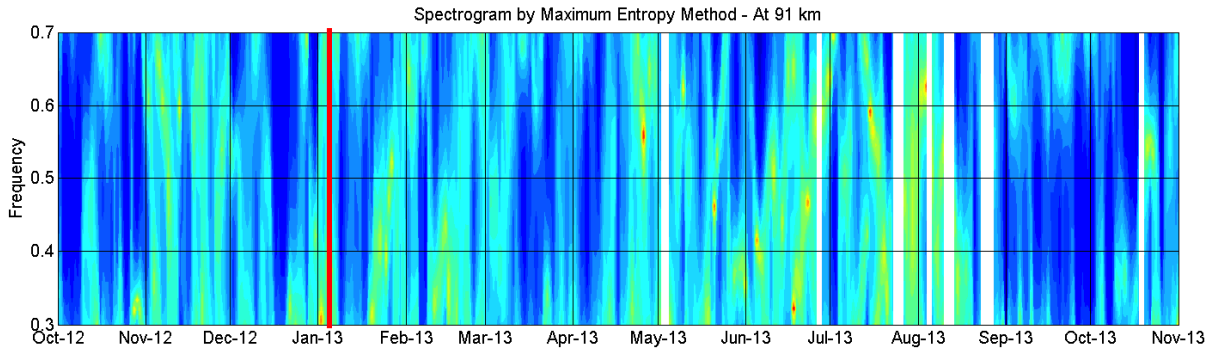

(b) Frequencyspectrum by (a) FFT and (b) MEM at 91 km

Figure A.3: Frequencyspectrum by (a) FFT and (b) MEM at 91 km

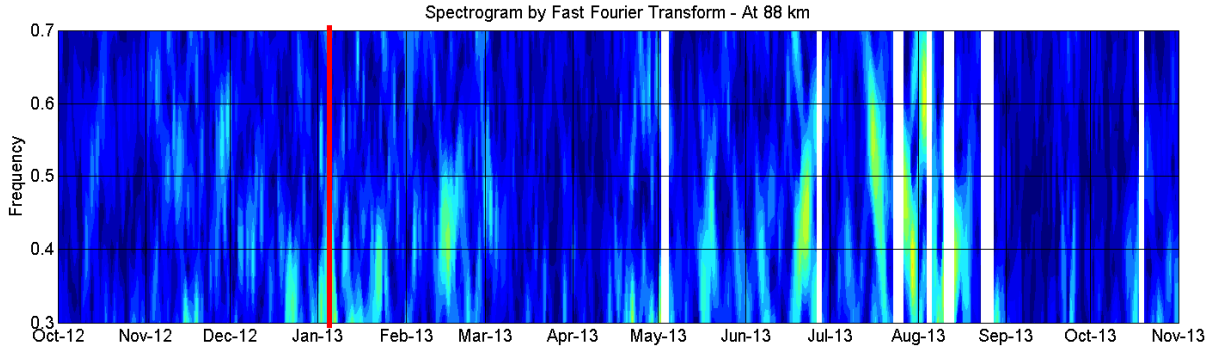

(a)

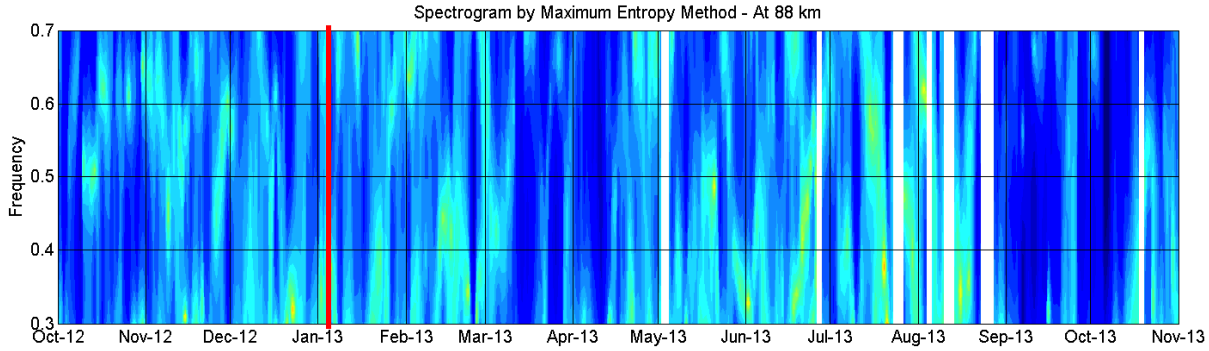

(b)

Figure A.4: Frequencyspectrum by (a) FFT and (b) MEM at 88 km

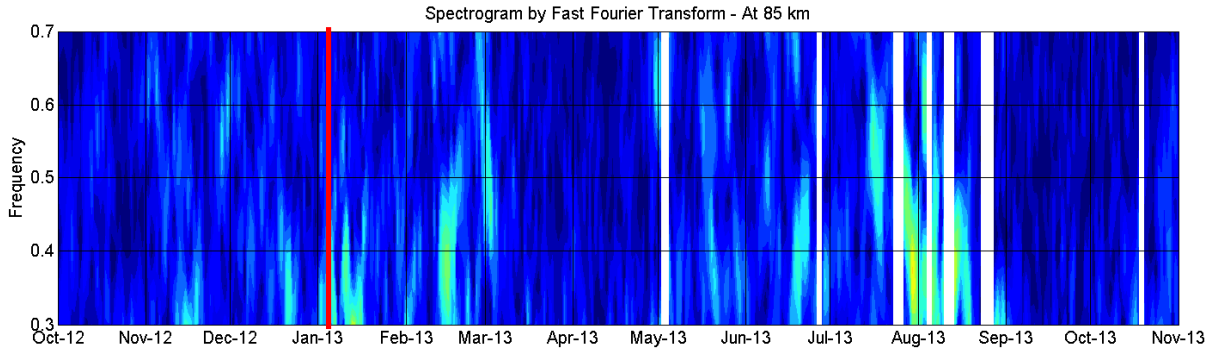

(a)

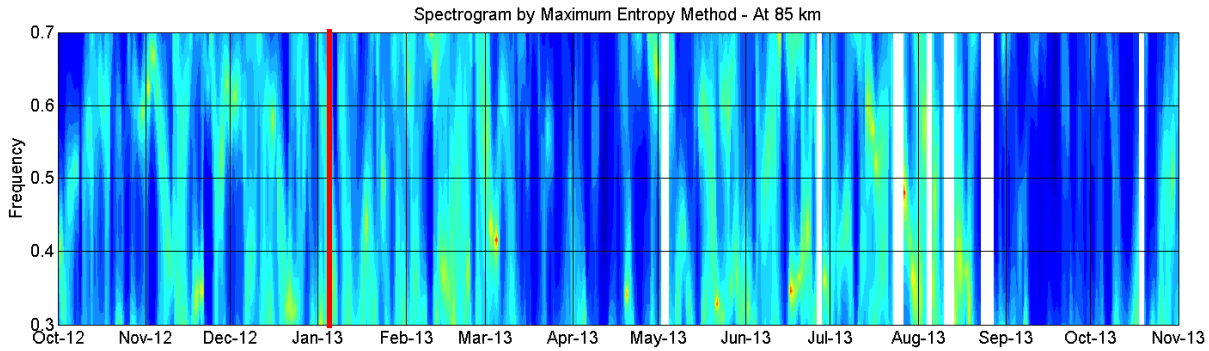

(b)

Figure A.5: Frequencyspectrum by (a) FFT and (b) MEM at 85 km

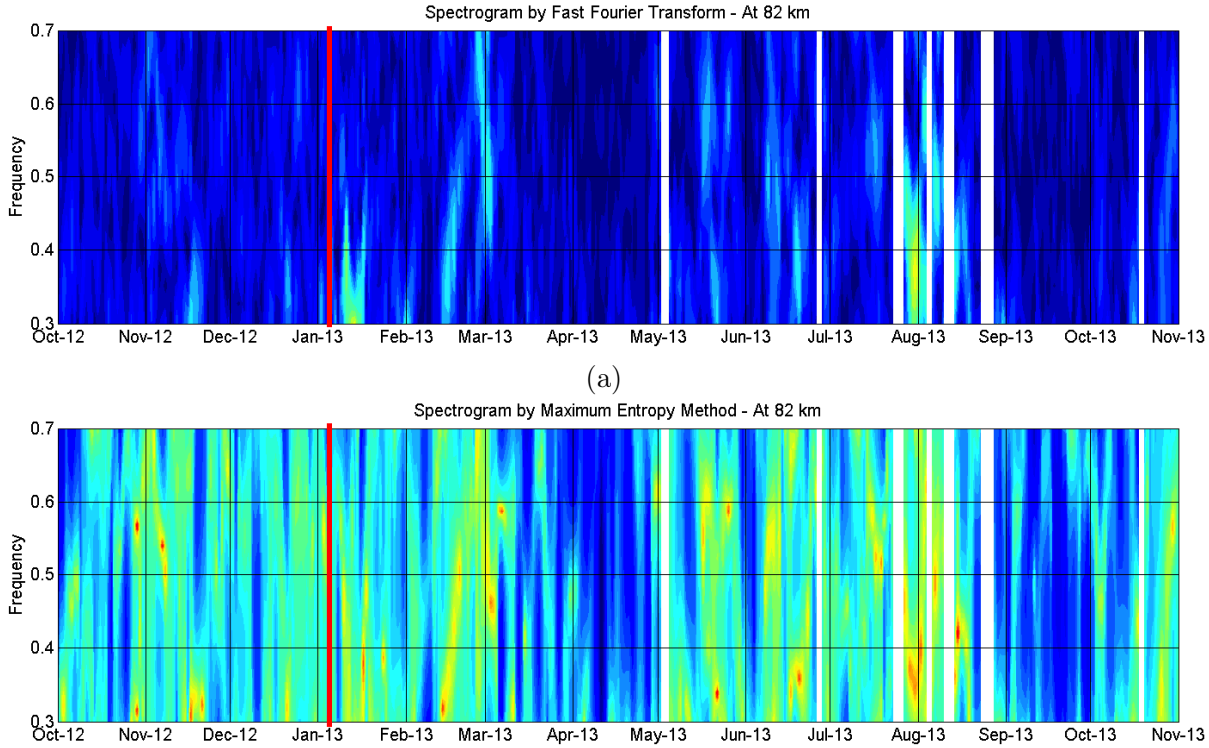

(a)

(b)

Figure A.6: Frequencyspectrum by (a) FFT and (b) MEM at 82 km

List of Figures

2.1 The conservation of absolute vorticity, leading to a westward propagating wave. Courtesy of Steve LaDochy, California state University. 9

2.2 (top) Original signal consisting of sine waves with periods of 5 days (0.2 cpd), 2 days (0.5 cpd), 1 day (1 cpd) and Gaussian white noise. (middle) The frequencyspectrum as computed by FFT (red) and MEM (blue). (bottom) MEM frequency spectrum using different numbers of Autocorrelation Coefficients (AC). 14

3.1 The SKiYMET radar set up as of Hocking et al. (2001) 16

4.1 Frequencyspectrum as computed by (a) FFT an (b) MEM. White fields are days of downtime by the radar and the red vertical line on 6th of january is the SSW event. Solstice is at mid-june. 18

4.2 4-day moving average zonal wind above Trondheim. Notice the strong wind shear at around 90km from mid january. Courtesy of Rosemarie de Wit, Norwegian University of Technology and Science. 19

4.3 The breakdown of the wintertime stratospheric vortex above Arctic 2013 near 35km. Note that our radarlocation (marked with a green dot) at Trondheim ($63°N$) is measuring only what happens above that location (Coy and Pawson, 2013) 20

4.4 Amplitude as a function of frequency, extracted out of data from october through mars. Moving average of amplitude at frequency binwidth of 0.006cdp. 21

4.5 Amplitude as a function of frequency, extracted out of data from april through september. Moving average of amplitude at frequency binwidth of 0.006cpd. 22

4.6 Occurrence of near 0.5 cpd frequencies, centered around the W3 mode, during (a) winter and (b) summer. The red line indicates the SSW event. 23

A.1 Frequencyspectrum by (a) FFT and (b) MEM at 98 km 26

A.2 Frequencyspectrum by (a) FFT and (b) MEM at 94 km 27
A.3 Frequencyspectrum by (a) FFT and (b) MEM at 91 km 27
A.4 Frequencyspectrum by (a) FFT and (b) MEM at 88 km 28
A.5 Frequencyspectrum by (a) FFT and (b) MEM at 85 km 28
A.6 Frequencyspectrum by (a) FFT and (b) MEM at 82 km 29

Bibliography

Andrews, D. G. (2010). *An Introduciton to Atmospheric Physics*. Cambridge University Press, Cambridge, 2 edition.

Baumgaertner, A., McDonald, A., Hibbins, R., Fritts, D., Murphy, D., and Vincent, R. (2008). Short-period planetary waves in the antarctic middle atmosphere. *Journal of Atmospheric and Solar-Terrestrial Physics*, 70:1336–1350.

Charney, J. G. and Drazin, P. G. (1962). Propagation of planetary-scale disturbances from the lower into the upper atmosphere. *Journal of Geophysical Research: Atmospheres*, 66(1):83–109.

Coy, L. and Pawson, S. (2013). Geos-5 analyses and forecasts of the major stratospheric sudden warming of january 2013. `http://gmao.gsfc.nasa.gov/researchhighlights/SSW/`.

Demissie, T. D. (2013). *The vertical structure and source regions of large and small scale waves in the middle atmosphere*. PhD thesis, Norwegian University of Science and Technology.

Fritts, D. C. annd Alexander, M. J. (2003). Gravity wave dynamics and effects in the middle atmosphere. *Reviews of Geosphysics*, 41(1):1003.

Hibbins, R. E., Espy, P. J., Jarvis, M. J., Riggin, D. M., and Fritts, D. C. (2007). A climatology of tides and gravity wave variance in the mlt above rothera, antarctica obtained by mf radar. *Journal of Atmospheric and Solar-Terrestrial Physics*, 69:578–588.

Hocking, W. K., Fuller, B., and Vandepeer, B. (2001). Real-time determination of meteor-related parameters utilizing modern digital technology. *Journal of Atmospheric and Solar-Terrestrial Physics*, 63:155–169.

Liou, K. N. (2002). *An Introduction to Atmospheric Radiation*. Academic Press, San Diego, California, 2 edition.

Nozawa, S., Iwahashi, H., Brekke, A., Hall, C. M., Meek, C., Man-son, A., Oyama, S., Murayama, Y., and Fujii, R. (2003). The quasi 2-day wave observed in the polar mesosphere: Comparison of the characteristics observed at tromsø and poker flat. *Journal of Geophysical Research: Atmospheres*, 108:4748.

Pancheva, D. (2000). Evidence for nonlinear coupling of planetary waves and tides in the lower thermosphere over bulgaria. *Journal of Atmospheric and Solar-Terrestrial Physics*, 62(2):115–132.

Plumb, A. R. (1982). Baroclinic instability of the summer mesosphere: A mechanism for the quasi-two-day wave? *Journal of the Atmospheric Sciences*, 40:262–270.

Press, W. H., Teukolsky, S. A., Vetterling, W. T., and Flannery, B. P. (1992). *Numerical Recipes in C - The Art of Scientific Computing*. Cambridge University Press, The Pitt Building, Trumpington Street, Cambridge, 2 edition.

Salby, M. L. (1981). The 2-day wave in the middle atmosphere: Observations and theory. *Journal of Geophysical Research: Oceans (1978-2012)*, 86(C10):9654–9660.

Salby, M. L. (1996). *Fundamentals of Atmospheric Physics*. Academic Press, San Diego, California, 1 edition.

Salby, M. L. and Callaghan, P. F. (2000). Seasonal amplification of the 2-day wave: Relationship between normal mode and instability. *Journal of the Atmospheric Sciences*, 58:1858–1860.

Tunbridge, V. M. and Mitchell, N. J. (2009). The two-day wave in the antarctic and arctic mesosphere and lower thermosphere. *Atmospheric Chemistry and Physics*, 9:6377–6388.

Walterscheid, R. L. and Vincent, R. A. (1996). Tidal generation of the phase-locked 2-day wave in the southern hemisphere summer by wave-wave interactions. *Journal of Geophsyical Research*, 101(26):567–576.

Zumdahl, S. S. and DeCoste, D. J. (2013). *Chemical Principles*. Brooks/Cole, Cengage Learning, 7 edition.